KOSZALIN UNIVERSITY OF TECHNOLOGY

RESEARCH AND MODELLING IN CIVIL ENGINEERING 2018

Edited by
Jacek Katzer, Krzysztof Cichocki and Jacek Domski

KOSZALIN 2018

MONOGRAPH NO 355
FACULTY OF CIVIL ENGINEERING,
ENVIRONMENTAL AND GEODETIC SCIENCES

ISSN 0239-7129
ISBN 978-83-7365-502-7

Chairman of the University Editorial Board
Zbigniew Danielewicz

Editors
Jacek Katzer, Krzysztof Cichocki and Jacek Domski
Koszalin University of Technology, Poland

Reviewers
Jacek Gołaszewski – Silesian University of Technology, Poland
Wojciech Sumelka – Poznań University of Technology, Poland

Technical editor
Czesław Suchocki

Website editor
Mariusz Ruchwa

Linguistic consultations
Ewa Sokołowska-Katzer

Typesetting
Czesław Suchocki

Cover design
Tadeusz Walczak

www.cecem.eu

KOSZALIN UNIVERSITY OF TECHNOLOGY PUBLISHING HOUSE
75-620 Koszalin, Racławicka 15-17, Poland

Koszalin 2018, 1st edition, publisher's sheet 13,42, circulation 120 copies
Printing: INTRO-DRUK, Koszalin, Poland

Table of contents

13. Comparison of pulse-echo-methods for testing of heat degradation concrete

Libor Topolář[1], Richard Dvořák[2], Michaela Hodoláková[3], Luboš Pazdera[4]

[1] *Brno University of Technology, Faculty of Civil Engineering, Brno, Czech Republic, orcid.org/0000-0001-9437-473X*

[2] *Brno University of Technology, Faculty of Civil Engineering, Brno, Czech Republic, orcid.org/0000-*

[3] *Brno University of Technology, Faculty of Civil Engineering, Brno, Czech Republic*

[4] *Brno University of Technology, Faculty of Civil Engineering, Brno, Czech Republic, orcid.org/0000-0002-9416-5644*

Abstract: The paper is focused on comparison of pulse-echo-methods for testing of heat degradation concrete. It was proven that the development of physico-mechanical and physico-chemical changes causes an uneven and stochastic increase of concrete heterogeneity and simultaneously a significant reduction of mechanical properties.

Keywords: pulse-echo, concrete, degradation

13.1. Introduction

The testing technology of composite materials used in the building industry has its specific characteristics when compared to other technical disciplines (engineering, electrical engineering, etc.). Most non-destructive acoustic measurement methods are well developed for homogeneous, especially basic metallic materials (steel, cast iron, etc.), but are not similarly well-developed for non-homogeneous materials. These non-homogeneous materials of course include building composites, either cement-based or alkali-activated (pastes, mortars, and concrete). That is the reason why it is very important to develop non-destructive defectoscopy testing methods. Non-destructive defectoscopy methods (defect imaging) are diagnostic methods that form an integral part of control processes of products, structures, and designs both in research, development, pre-production and manufacturing stages, as well as in real-life applications. Without defectoscopy, it would not be possible to provide error-free operation, reliability, and safety in many areas such as aviation, nuclear power, chemicals, as well as safety of bridges, dams, etc. In general, non-destructive defectoscopy deals with the testing of the structure of metallic and non-metallic materials and internal or surface defects of objects without

compromising their integrity. Material and product defects include incorrect chemical composition, structural defects, deviations from the specified mechanical and physical properties, non-homogeneity (cracks, tears), cavities (bubbles, pores, precipitates), inclusions (slag, non-metallic and metallic inclusions), shape defects, corrosion, wear, etc. (Kreidl, 2006). Non-destructive defectoscopy testing methods are based on different physical principles and utilize specific material properties. Individual procedures vary in demands on technical equipment and personnel qualifications and it is impossible to establish only one generally valid procedure for the detection of defect. The use of a particular method always depends on the given situation. There is no ideal universal defectoscopy method for the control of specific components or materials. The choice of the optimal method or a combination of methods depends on the particular application, material, etc. A combination of several different methods and procedures are therefore commonly used to determine the most accurate information for the given case. This chapter will deal with pulse-echo methods and the method of the maximum length sequence (MLS).

13.1.1 Principle of Impact and Pulse-echo methods

The Impact-echo (IE) method, often referred to as "indirect" acoustic emission, uses an external source of the acoustic signal. The term hammer method is also used and usually employs a mechanical impulse as the signal transmitter– a hammer stroke, or the fall of a steel ball (Fig. 13.1 and Fig. 13.2). This method deals with a response, where we monitor the parameters of the signal that has been transformed by the passage through the material and recorded on the surface of the examined sample (Malhotra and Carino, 2004; Kopec, 2008). The Impact-echo method is based on the analysis of the response of a mechanical impulse that creates harmonic waves in the studied object at its natural frequency and at higher harmonic frequencies. These frequencies primarily depend on the dimensions and material characteristics of the tested object. A transient stress pulse applied to the surface creates elastic waves in the material, which further propagate through the material by spherical wavefronts as longitudinal and transverse waves and is superimposed by reflected waves from the outer surfaces as well as from internal defects (inconsistencies, non-homogeneities, cavities, micro and macro cracks, etc.).

These waves are transformed on the surface of the sample into surface waves, also called Rayleigh's, respectively Lamb waves, which are then recorded and evaluated. The recorded response indicates the existence of structural defects, but does not specify the type of the defect or its shape and size (Kořenská, 2006).

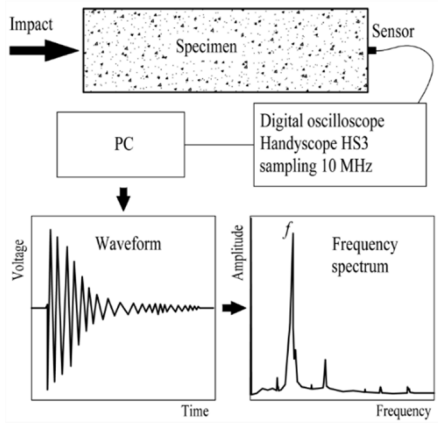

Fig. 13.1. Schematic representation of the Impact and Pulse-echo methods

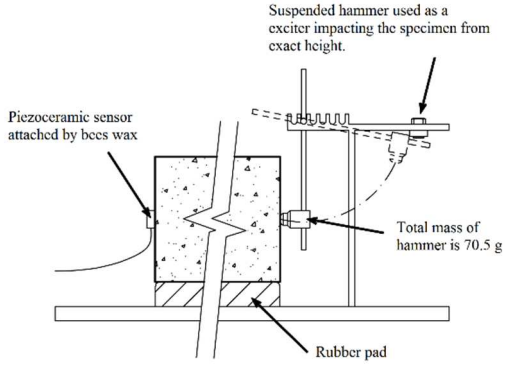

Fig. 13.2. The method of signal transmission with a hanging hammer for the Impact-echo method

For impact and pulse-echo methods, the source of the stress impulse applied to the surface of the tested object may be a mechanical impulse or a generated signal. If a mechanical impulse is used for the testing, we talk about the Impact-echo method and if the generate the mechanical wave by a generator, we talk about the Pulse-echo method (Carino, 2001). The generated signal may be in the form of a pulse or a continuous noise or harmonic signal (Malhotra and Carino, 2004; Domain, 2007). The evaluation of the response signals to the transmitted pulse in the tested object can be performed in two basic systems of analysis. In

the first case, the resulting shift in relation to time is evaluated, and in the second case, the signals are converted to the frequency domain and a frequency analysis is performed. The frequency analysis is used more often, where the examined signal is converted from the time domain to the frequency domain with the Fourier Transform, most frequently with the fast Fourier Transform (FFT - Fast Fourier Transform). The Fourier Transform decomposes the signal into many sine waves of different frequencies (Domain, 2007) and thus generates a spectrum of amplitudes depending on the frequency. The individual peaks corresponding to the dominant frequencies indicate the depth of the boundary surfaces of the object or also the depth of the interface on the surface of the cracks and cavities or the depth of the interface between two materials of different acoustic impedances.

13.1.2 The principle of the MLS method

Scientists involved in vibroacoustics have been trying to reduce the noise caused by the transmitted signal in pulse-compression methods. The MLS method was developed for this particular purpose (Fig. 13.3). Instead of transmitting one short impulse in the test sample (whether by a hammer stroke, or a piezoelectric transmitter), it is transmitted by a pseudorandom binary signal (working with only two levels of voltage), which is generated into a continuous chain of the transmitted signal. During recording of the impulse response (IR – "impulse response"), the start and the end of the transmitted signal are not relevant. Due to the nature of the MLS signal, the evaluation algorithm can select any point in the signal, select a sequence of points of the length of the partial transmitted signal and obtain precisely one impulse response. The advantage of this approach is that we can create up to 2^{16} transmitted impulses hidden in one maximum length sequence in a relatively short time interval of a few seconds. By subsequent averaging of each FFT calculated from the partial IR, we obtain a much more accurate impulse response than in the case of the common IE method. This allows a substantial reduction of the quantization noise on the side of the generator, a reduction of the hardware costs, and a reduction of the influence of non-linearities (Lam and Hui, 1982).

MLS can be used in a wider frequency range than in case of the IE method, which works primarily in the low frequency range to 30 kHz. The generation of the transmitted signal can be done by a piezoelectric transmitter or contact speakers with different threshold voltage of the transmitted MLS signal. In this area, we can also speak about a linear and non-linear response of the test specimen (Potchinkov, 2005).

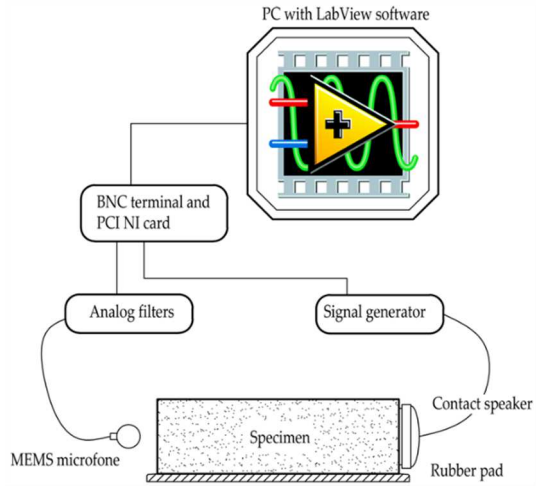

Fig. 13.3. Schematic representation of the use of the MLS method

Thanks to the possibility of transmitting the MLS signal with different threshold voltage, it is possible to record the shift of its natural resonance frequency f at maximum oscillation and the frequency f_0 at minimum oscillation. The proposed method allows both the interpretation of the measured transmitted signal in the frequency domain and the assessment of the parameter α characterizing the non-linear nature of the tested specimen, which is given by the equation (Carbol, 2016):

$$\alpha = \frac{\Delta f}{f_0} = \frac{f - f_0}{f_0} \tag{13.1}$$

13.2. Materials and experimental setup

A total of 30 test specimens with dimensions of 0.1 × 0.1 × 0.4 m were produced from two mixtures B and C. Each mixture was divided into five temperature sets, one reference set was kept at 20 °C and the remaining sets were divided into individual firing temperatures 400, 600, 800 and 1000 °C. The composition of the mixtures used during the experiments is given in Tab. 13.1. All the samples were kept in a water bath for 28 days. Each test specimen was pre-dried in a laboratory oven at 110 °C for 72 hours. This procedure removed free water from the specimens and consequently spalling of the specimens (Zhao *et al.*, 2014) at temperatures above 400 °C. During firing, the temperature in the oven was set to at an increase of 5 °C/min and the target temperature was then maintained for one hour. The specimens then cooled freely with access to air in the oven to the laboratory temperature.

Table 13.1. Mixture design

Compounds	Amount of each compound for 1 m^3 in kg	
	Set B	Set C
Cement CEM I 42.5 R	345	
Mix water	173	176
Superplasticizer Sica Viscocrete 2030	2.5	3.1
Fine aggregate Žabčice 0/4 mm	896	813
Coarse aggregate Olbramovice 4/8 mm	–	1010
Coarse aggregate Olbramovice 8/16 mm	521	–
Coarse aggregate Olbramovice 11/22 mm	391	–

When the signal is transmitted by a mechanical stroke, the hammer is suspended in a horizontal position. To transmit the impulse, it is released and therefore always falls from the same height (Fig. 13.2). In such a situation, it is possible to compare the amplitudes from individual measurements. Tests using the Impact-echo method consist of the first phase of the transmission and recording of the signal using a sensor (DAKEL IDK-09) and oscilloscope (HandyScope HS3), its conversion to a frequency spectrum using FFT and subsequent analysis of the dominant frequencies.

For the pulse-echo method, the pulse generator (Agilent 33220a) was set to the following output values: period 5s; amplitude 10 V_{pp}; pulse width 500 μs. These pulse signals were captured after passing through the sample by the piezoelectric sensor (DAKEL IDK 09) and then amplified with a preamplifier (AS3K 433) with a gain of 35 dB and subsequently recorded by the DAKEL XEDO device where they were again amplified if necessary by internal circuits.

The MLS measuring device is automated and consists of the transmission of the pseudo-sequence signal, non-contact recording of the vibration of the test specimen subjected to transmission using a highly sensitive MEMS microphone and vibration decrease and subsequent automatic analysis of the recording. A single test cycle contains three parameters which characterize the linear and nonlinear behaviour of the sample - the resonance frequency f, the non-guaranteed sound velocity in the material v_u and the parameter α characterizing the non-linear character. The use of the pulse compression of the signal is quite unusual in the construction industry. Only recently has the frequency of this issue increased in professional journals. A great potential lies in the mentioned combination of three test methods into one, in high test rate and repeatability of measurements, but also in the theoretical possibility of testing massive elements (Carbol, 2016).

13.3. Achieved results in time and frequency domain for each method

13.3.1. Results from the Impact-echo method

Examples of the recorded signals are shown in Fig. 13.4 Several basic characteristic signs of the tested material are distinguishable from the graphs. In both cases applies that the specimens degraded at the temperature of 1000 °C have a lower frequency than non-degraded specimens. In addition, the reference set of the B mixture exhibits a substantially discontinuous decrease of individual oscillations in comparison to the almost continuous attenuation in case of the C mixture.

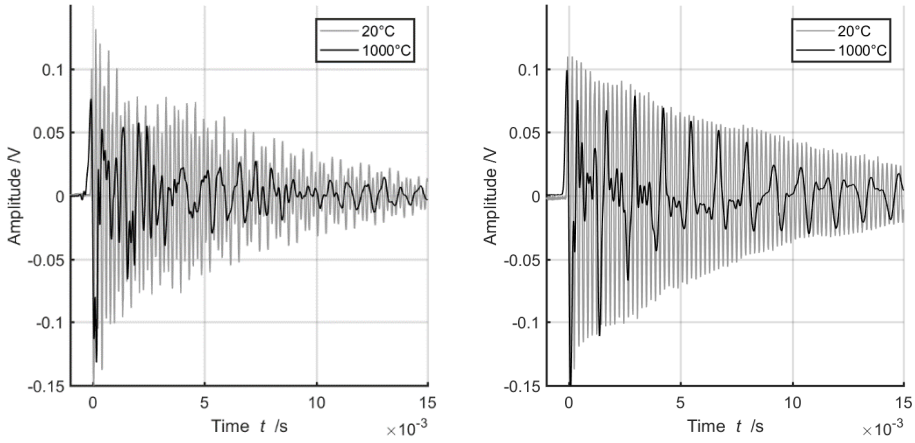

Fig. 13.4. An example of a signal from the IE measurement of the test specimens (left – mixture B, right – mixture C)

When comparing the amplitudes, we can observe a more pronounced difference in the course of the amplitude of the degraded sets of both the mixtures. In case of firing to 1000 °C, the signal of the mixture B exhibits some inconsistencies; the signal of the mixture C has a harmonic character.

These differences are noticeable when comparing the FFT of the individual temperature sets from the B mixture shown in Fig 13.5 and the C mixture shown in Fig. 13.6.

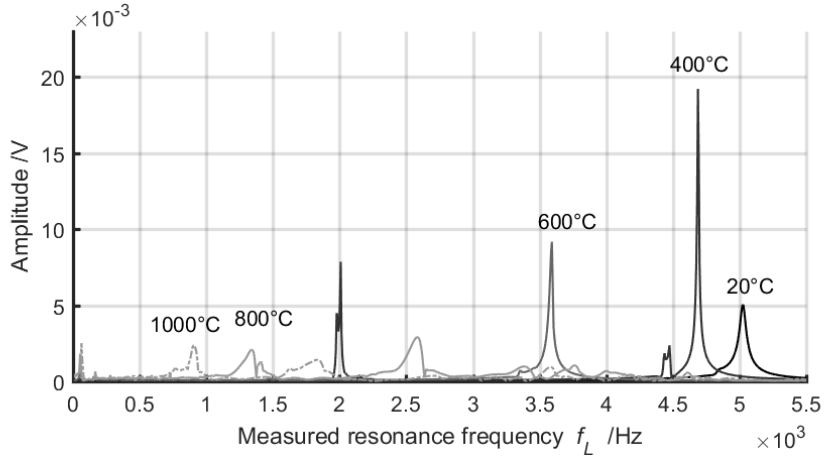

Fig. 13.5. Resonance frequency of the mixture B test specimens

These are selected representative frequency spectra from each temperature set and do not include all the conducted measurements. Besides the frequency shift of the resonance frequency between the individual temperatures, which is evident on both graphs, both mixtures have different amplitude of the measured frequencies. The amplitude of the mixture C is up to twice that of the mixture B. From 800 °C, the peaks of the resonance frequencies of mixture B exhibit a slight flattening due to a higher degree of noise as seen in Fig. 13.4 (left).

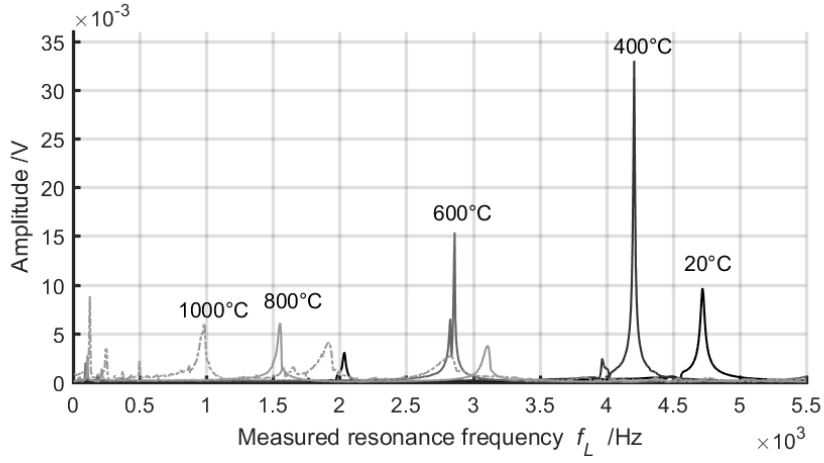

Fig. 13.6. Resonance frequency of the mixture C test specimens

Since both mixtures differ only in the amount of the coarse aggregate (Tab 13.1.), we can attribute these differences to the used aggregate and the overall behaviour of the used materials at high temperatures. While the basically fine-grained mixture C has a high response in all temperature sets, the mixture B behaves like a less compact material and dampens the mechanical impulse to a higher degree.

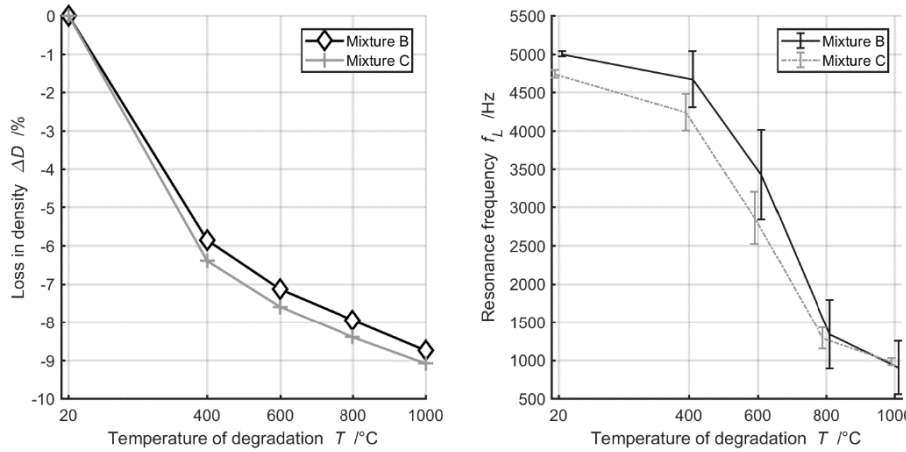

Fig. 13.7. Relative density loss of the tested sets (left graph), average resonance frequency of longitudinal waves of mixtures B and C (right graph)

The change in the resonance frequency of the test specimens in the longitudinal direction of testing indicates the most significant change in the residual physical-mechanical properties of the tested mixtures. Both mixtures reach their reference resonance frequencies from 4.7 kHz to 4.9 kHz with little variance of the values, as shown in Fig. 13.7 (right). The change in frequencies for specimens fired to 400 °C is not so significant when compared to other temperatures, but demonstrates the effect of the present physically and chemically bound water. The physically bound water escapes in the form of steam from the plain concrete at around 100 to 180 °C, and at the critical temperature of 374 °C, the chemically bound water can no longer be present (Hager, 2004). The mixture B reaches a reduction of 6% in this case and the mixture C of up to 10%. Since the measured amplitudes of the 400 °C temperature set for both mixtures exhibit the highest measured amplitude of the resonance frequency, it can be concluded that from the point of degradation, the test specimens were not significantly damaged by the elevated temperature, but the decrease in the frequency is caused by the escaping physically and chemically bound water. Fig. 13.7 (left) shows a decrease in the density of the

tested sets in relation to the degradation temperature. As can be seen, the most significant decrease of 6% is between 20 °C and 400 °C, the rest of the stress temperatures influenced the density by only 3%. In the frequency domain, however, this change corresponds to the main decrease in the resonance frequency and the most significant degradation of both mixtures.

Another interesting behaviour of the tested mixtures was demonstrated on the variance of the measured values. Fig. 13.7 (right) shows the probable error of the arithmetic mean of the measured values presented by error bars. The mixture B exhibits relatively high accuracy only for the reference set, the other measurements of the temperature sets are marked by a relatively large error, which is true up to 1000 °C. The variance of the measured values for mixture C, however, decreases with the increasing temperature stress up to the 1000 °C level, where the error in the mean is almost identical to the reference set.

From the point of view of the cementitious matrix, gradual decomposition of portlandite $Ca(OH)_2$ and CSH gels occurs between the temperature of 400 °C and 600 °C and is accompanied by general shrinkage of the cementitious matrix and the first significant formation of cracks on the interface of the filler and binder. On the other hand, quartz components of the material, which mostly form the filler, and are mostly composed of β-quartz, feldspar and mica, experience expansion and cracking of the quartz aggregate. From around 780 °C to 920 °C, gradual decomposition of fine-grained and coarse-grained carbonates $CaCO_3$, and CO_2 occurs and results in their thermal decomposition to CaO and CO_2, which further contributes to the density loss as well as to the main shift of the resonance frequencies to a lower frequency domain (Bodnárová, 2013).

13.3.2. Results from the Pulse-echo method

The graphs in Fig. 13.8. include the records of the signals in the time domain for both sample mixtures and two selected temperatures. The vertical axis represents the actual amplitude (the total gain has been taken into account) of the individual signals and the horizontal axis represents time. The upper graphs show

a comparison between the two sets for reference samples (20 °C). Both graphs demonstrate the typical pulse signal that has passed through the sample without significant inconsistencies or defects. The larger amount of the fine aggregate of the mixture C probably caused the lower recorded amplitude of the signal. The situation is dramatically different in case of the selected firingtemperature (600 °C). The recorded signal is highly attenuated and also greatly distorted. A better picture of the signal attenuation in the time domain is given in Fig. 13.9.

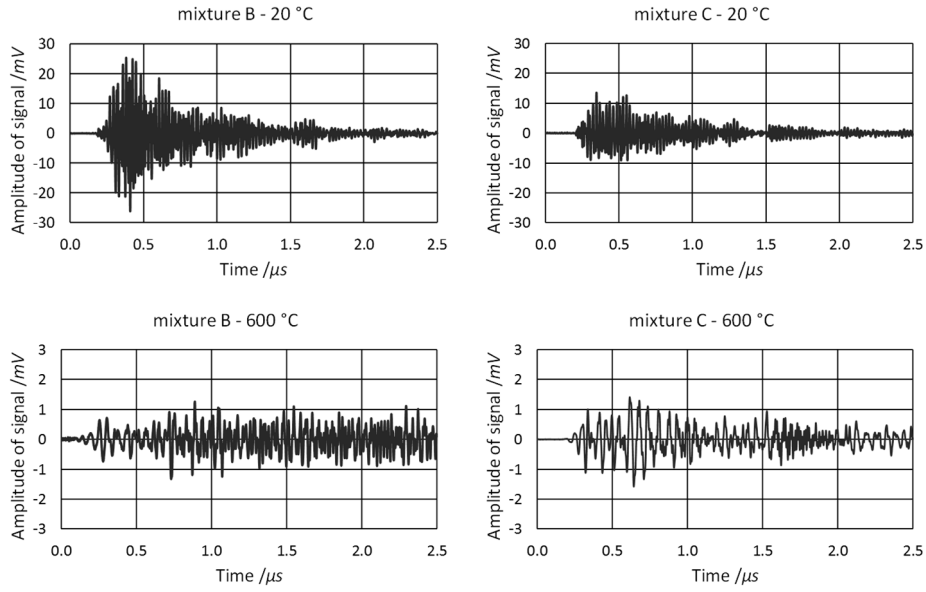

Fig. 13.8. Examples of the signal in the time domain from the Pulse-echo method measurements

The graph in Fig. 13.9 shows the decrease in the signal amplitude for individual firing temperatures. The higher amplitude of the degraded samples (200, 400, 600, 800 and 1000 °C) indicates a greater sensitivity of the internal structure, i.e. smaller damage due to elevated temperatures. In this respect, the mixture C samples seem to be better since the amplitude values are higher for all the temperatures, although in case of some temperatures only insignificantly.

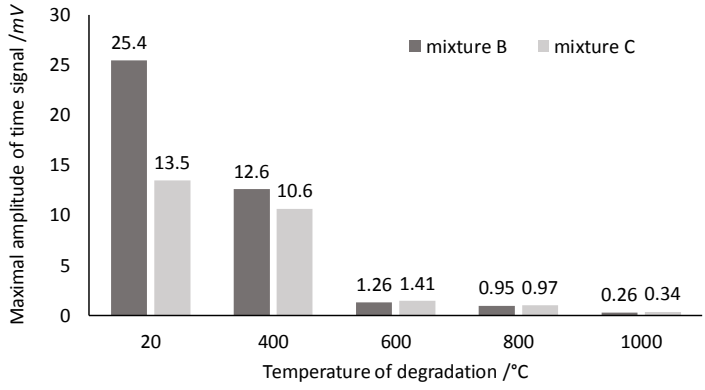

Fig. 13.9. Decrease in the signal amplitude in the time domain for mixture B and C

The graphs in Fig. 13.10 present the records of the signal for both mixtures and selected temperatures (reference and 600 °C) in the frequency domain. By comparing individual sets in different temperatures, it is evident that after firing to 600 °C, the dominant frequency shifts towards lower values, i.e. to the left in the frequency spectrum. It can therefore be assumed that lower frequencies indicate higher structural damage of the individual samples. It can also be seen that in addition to the dominant frequency, other significant frequencies occur in the degraded samples, which are not so apparent in the reference samples. The change of the dominant frequencies for both mixtures and all degradation temperatures is summarized in graph (Fig. 13.11).

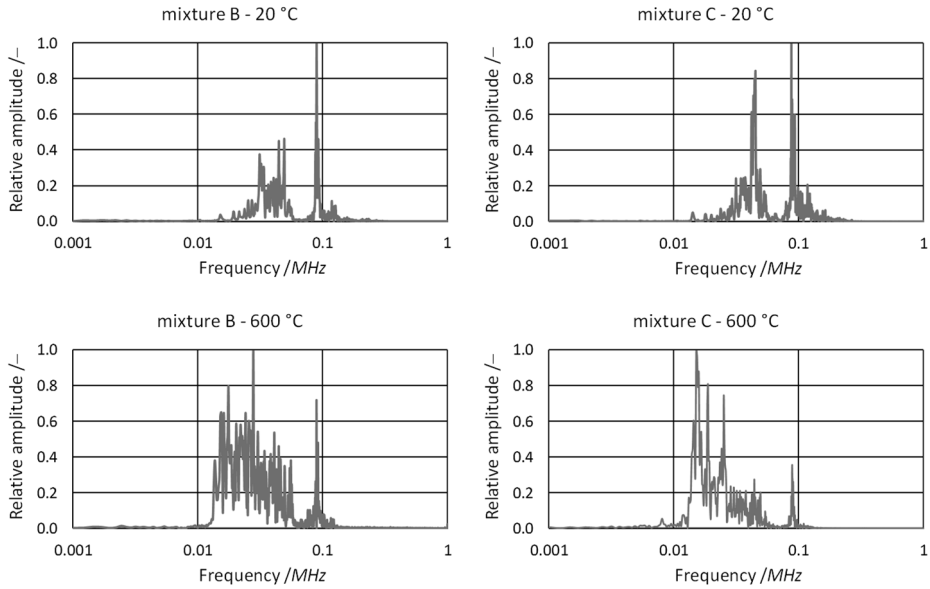

Fig. 13.10. Examples of recalculated signals in the frequency domain from the Pulse-echo method measurements

The summary graph shows the shift of the dominant frequency positions to lower values, which again indicates greater damage and structural changes. Compared to the maximum amplitudes from the time domain, there is a slight difference at temperatures of 600 and 800 ° C, when the samples first exhibit crystalline changes and consequently the decomposition of Portlandite. This is probably connected to the larger amount of the fine aggregate (cement grains are closer to each other and the change in the Portlandite structure therefore occurs) in samples from the C mixture, which then leads to larger shifts of the dominant frequency positions than in case of the mixture B samples.

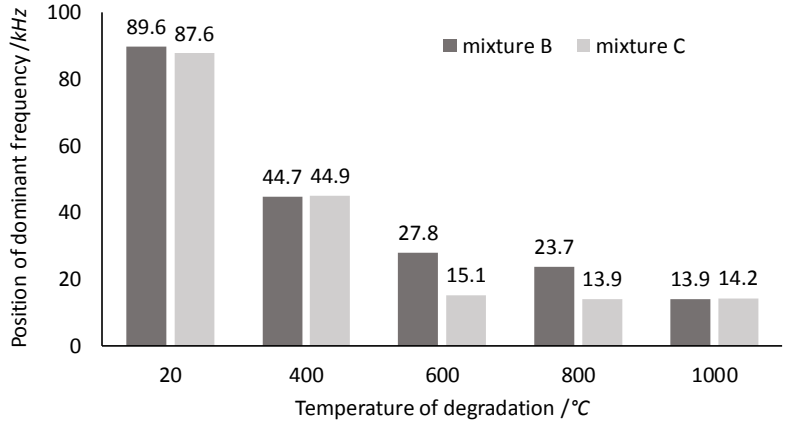

Fig. 13.11. A change of the position of the dominant frequencies for mixtures B and C

13.3.3. Results from the MLS method

The resulting frequency spectra obtained with the MLS method exhibit significantly greater response on particular resonance and harmonics frequencies (Fig 13.12 to 13.17). All the measured spectra are created using three threshold transmission voltages 8 V, 16 V and 24 V. The sequence length of the maximum length was set to 17 bits with the generating frequency of 100 kHz. The sample response was read with a sampling frequency of 1 MHz. A Sono gel was used as a coupling medium between the speaker and the test specimen, and the response of the specimen was recorded by a sensitive MEMS microphone through air. The LabView software from National Instruments was used to evaluate the measured response (Carbol, 2015). The tested specimens of mixture B and C can therefore be evaluated on a wider frequency spectrum of up to 30 kHz. When compared to IE, the individual peaks are considerably sharper. The created spectra for the reference samples allow clear detection of the first dominant resonance frequency and then its subsequent harmonic frequencies, both for the mixture B in Fig. 13.12. as well as for the mixture C in Fig. 13.15. The measured resonance frequencies match the frequencies obtained using the IE method with maximum differences in single percentages. The measured values of the individual temperature sets of both mixtures are presented in table Tab. 13.2.

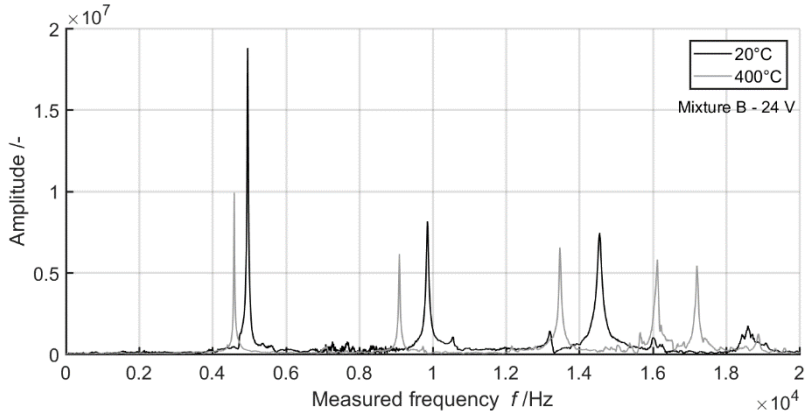

Fig. 13.12. The frequency spectrum of the mixture B obtained by MLS testing (20 °C and 400 °C)

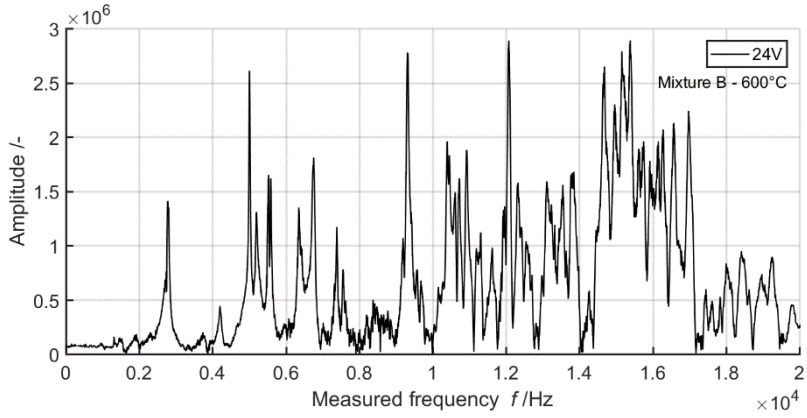

Fig. 13.13. The frequency spectrum of the mixture B obtained by MLS testing (600 °C)

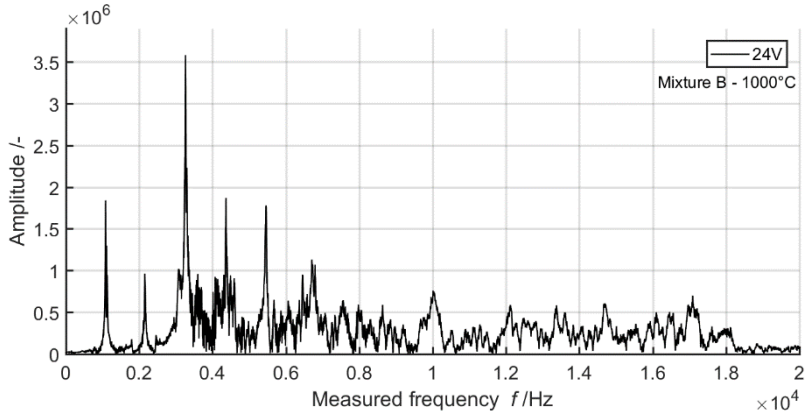

Fig. 13.14. The frequency spectrum of the mixture B obtained by MLS testing (1000 °C)

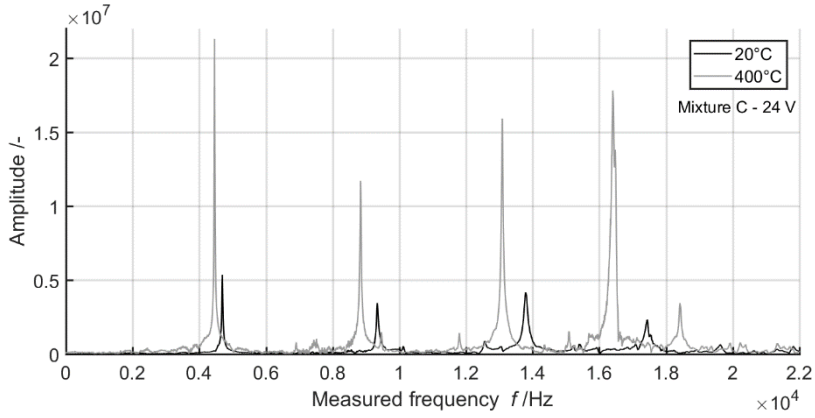

Fig. 13.15. The frequency spectrum of the mixture C obtained by MLS testing (20 °C and 400 °C)

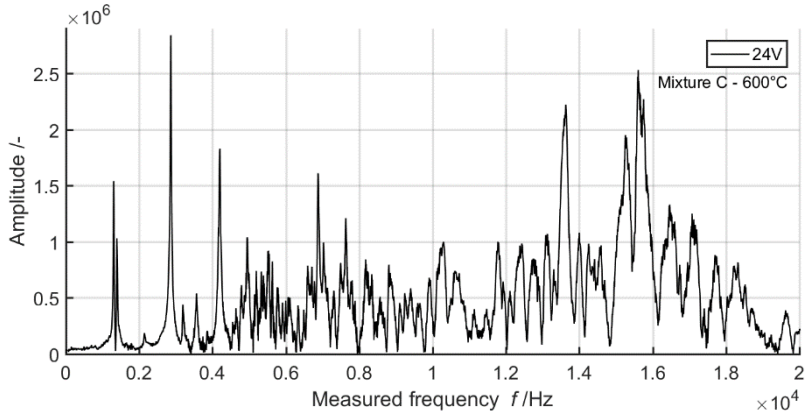

Fig. 13.16. The frequency spectrum of the mixture C obtained by MLS testing (600 °C)

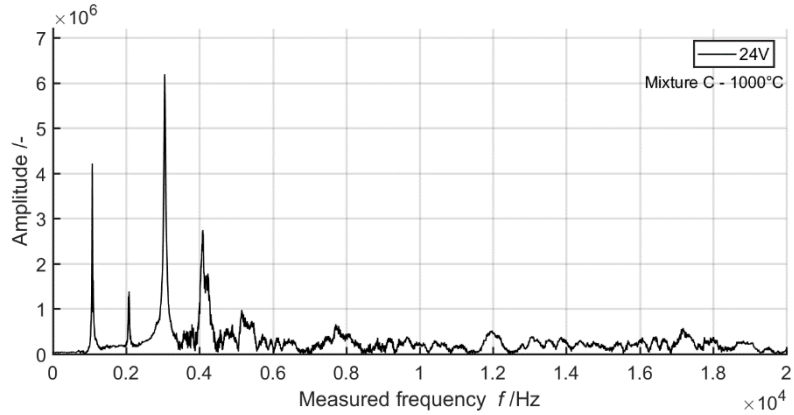

Fig. 13.17. The frequency spectrum of the mixture C obtained by MLS testing (1000 °C)

To be more understandable, the graphs Fig. 13.12 to 13.17 were generated only from a part of the frequency spectrum transmitted by the signal with the threshold voltage of 24 V. All three voltages are shown in graphs 13.18, which illustrate the linear and non-linear character of the temperature sets.

With increasing temperature degradation, the rate of the signal noise increases. The way in which the MLS method creates individual frequency spectra allows a higher response on the resonance frequencies of the tested material. MLS testing achieves much more pronounced results especially when compared to the IE method.

Graphs 13.12 and 13.15 compare the change of the frequency spectrum between the set of 20 °C and 400 °C. While firing to 400 °C in case of the mixture B caused a slight shift of the resonance frequency and a decrease in the response of the amplitude, there was an increase in the response amplitude in case of the mixture C. Only mixture C therefore corresponds to the development of the amplitude obtained during IE testing. As has been mentioned above, the IE method, in the initial firing phase of up to 400 °C, is most influenced by the physically and chemically bound water in the tested mixtures. The first dominant resonance frequencies are easily recognisable up to 1000 °C.

In case of the reference sets, we can also observe decreasing amplitude of the harmonic frequencies. The monitoring of the harmonic frequencies of non-linear ultrasonic testing of concrete can determine the presence of an internal defect. Looking at the resonance frequencies and the first three harmonic frequencies, we find a similar development in this case as well (Ongpeng, Oreta and Hirose, 2015).

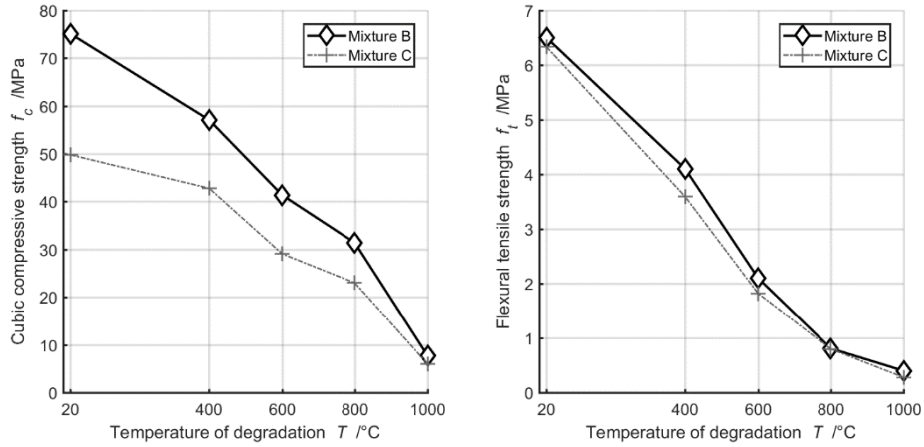

Fig. 13.18. Average compressive (left) and tensile strength (right)

In case of mixture B and C for the temperature sets of 20 °C, the first dominant frequency exhibits the highest amplitude and the other harmonic frequencies have decreasing amplitudes. For temperature sets of 600 °C and 1000 °C, the amplitudes change and the first dominant frequency have a lower amplitude than its following harmonic frequencies. Due to the knowledge of the residual physical-mechanical properties, which were described in graphs 13.19 to 13.20, we can state that the changes obtained with non-destructive methods in the

tested material correlate with the destructive tests and in particular with the compressive and tensile strengths.

The strengths of the tested mixtures correspond to the used material composition. The mixture B containing coarse aggregate 8/16 mm and 11/22 mm achieves the highest strengths in both compressive and tensile tests. With gradual degradation, however, its compressive and tensile strengths gradually approach the mixture C until they reach almost the same value at the degradation temperature of 1000 °C. This indicates that the temperature of 1000 °C is the material minimum for both tested mixtures.

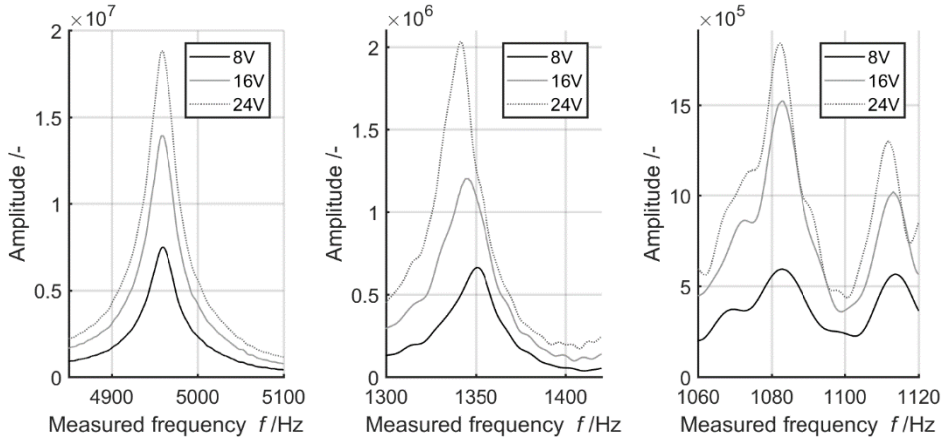

Fig. 13.19. Progress of the linear character (left and right) and the non-linear character (centre) of the resonance frequency of the mixture B temperature sets: 20 °C (left), 800 °C (centre), 1000 °C (right)

Looking at the graphs 13.19 to 13.20, we can observe the linear and non-linear character of the tested mixtures. For illustration purposes, we selected the peaks of resonance frequencies of the temperature sets which allow the non-linearity phenomenon to be recognized to the greatest and smallest extent.

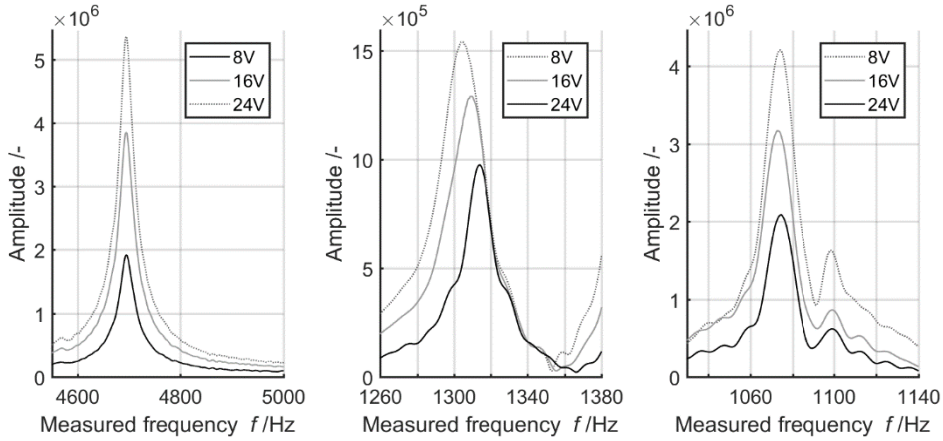

Fig. 13.20. Progress of the linear character (left and right) and the non-linear character (centre) of the resonance frequency of the mixture C temperature sets: 20 °C (left), 800 °C (centre), 1000 °C (right)

In practice, almost all materials behave non-linearly, i.e. the stress induced inside the system is non-linearly dependent on strain, and after unloading, it returns to the initial state with persisting plastic deformation. The linearly behaving system, on the other hand, returns to their initial state after unloading without losses of the internal energy – it therefore behaves elastically (Ongpeng, Oreta and Hirose, 2015; Lexcellent, 2017). The non-linearity parameter α was observed in the tested sets and is presented in Tab. 13.2. All the tested sets exhibited the non-linear character, to the lowest extent in case of the B mixture temperature set 20 °C and to the highest extent in case of the temperature set 800 °C of the same mixture. In case of mixture C, non-linearity was manifested to a lesser degree. In the frequency spectrum outside the dominant peaks, skipping of the frequencies between the 8, 16 and 24 V voltage thresholds was also observed. While the graphs 13.19 and 13.20 present gradually increasing amplitudes in the same order as in which the individual signals were chronologically transmitted, other places may show changes in the order. The extent of this phenomenon, however, diminishes in the resonance frequency domain. Overall, the test specimens produced from the mixture C appear to be less usable at high temperatures, but as a substantially more stable material with respect to the measured parameters. This result confirms both the measured values from the evaluation using the Impact-echo method as well as using the MLS method.

Table 13.2. Results obtained from MLS measurement of mixture B and C

Mixture	T /*°C*	v_L /ms^{-1}	f /*Hz*	f_0 /*Hz*	$\alpha \times 10^4$ /–
Mixture B	20	4645	5000	5001	1.50
	400	4089	4671	4671	1.71
	600	2597	3425	3425	30.76
	800	1412	1341	1339	137.00
	1000	975	905	904	99.90
Mixture C	20	4300	4739	4740	2.80
	400	3513	4240	4239	2.36
	600	2429	2863	2863	17.44
	800	1394	1289	1301	33.50
	1000	678	981	978	26.72

13.4. Comparison of achieved results and discussions

Tab. 13.3 presents a comparison of the average values of the dominant frequencies (f_L – impact-echo; f_0 – MLS; f_{PE} – pulse-echo) of the individual methods including their relative errors. The results in Tab. 13.3 can be interpreted from several points of view:

- In regard to the degree of degradation, it is evident that the lowest relative error values are for specimens that were not degraded. The highest variance of the measured values, on the other hand, was obtained for specimens fired at 600 °C. This development of physico-mechanical and physico-chemical changes causes an uneven and stochastic increase of concrete heterogeneity and simultaneously a significant reduction of mechanical properties. Healthy concrete consists of clearly defined materials and its response to an excited signal is unambiguous. Degraded concrete consists of healthy components, partly degraded or completely degraded components, but also of new phases that are still forming in the material during the firing process.
- Within the ability of the individual methods to provide accurate results, we can describe differences in the accuracy of the measured quantities from the point of view of the application of the test procedure itself. The impact-echo method is dependent on a stroke of a spherical hammer, where the same initial conditions cannot be ensured for each test (the place and force of the impact of a hammer). The MLS method, which employs a sensitive microphone as a receiver and a contact

speaker as an exciter, receives the response of the specimen to an excited signal influenced by the ambient noise (background laboratory acoustic conditions). The lowest relative error values are therefore reached by the pulse-echo method. This result is due to the character of the test assembly with the piezoceramic exciter and the receiver being attached to the surface of the test specimen and the specimen being excited by longitudinal waves at higher frequencies (above 20 kHz). This method is therefore able to ensure the highest homogeneity of the excited signal and therefore the response of the specimen to the excited signal.

From the point of view of the destructive tests (Table 13.4), it can be observed that while mixture B reached the compressive strength of up to 75 MPa and can therefore be considered high performance concrete, the mixture C achieves slightly higher compressive strengths than ordinary concrete but does not exceed 50 MPa. However, the subsequent decreasing trend in the strengths linked to temperature degradation is very similar for both mixtures. The lowest values of mechanical properties were recorded for temperature sets degraded at 1000 °C. At this state, the decomposition of all the key hydraulic components, which ensure internal cohesion and strength of cement composites, has taken place and the material itself had a strong tendency to crumble and cracked.

Table 13.3. Results of non-destructive acoustic tests of mixture B and C

Mixture	T /°C	f_L /Hz	$\delta(f_L)$ /%	f_0 /Hz	$\delta(f_0)$ /%	f_{PE} /kHz	$\delta(f_0)$ /%
Mixture B	20	5000.25	0.17	5000.50	0.21	89.6	0.32
	400	4624.01	1.39	4670.60	1.70	44.7	0.22
	600	3192.21	5.89	3425.20	3.55	27.8	5.57
	800	1263.49	2.85	1339.20	1.32	23.7	2.52
	1000	744.72	3.19	904.08	3.68	13.9	2.63
Mixture C	20	4958.19	0.43	4740.33	0.37	87.6	0.11
	400	4172.22	2.42	4239.00	1.85	44.9	0.11
	600	2805.22	4.77	2862.80	4.11	15.1	0.37
	800	1365.12	2.68	1301.00	2.37	13.9	0.12
	1000	788.78	2.73	978.00	3.13	14.2	0.23

Table 13.4. Results of destructive tests of mixture B and C

Mixture	T /°C	f_c /MPa	$\delta(f_c)$ /%	f_{ct} /MPa	$\delta(f_{ct})$ /%
Mixture B	20	75.10	1.02	6.50	0.27
	400	57.10	1.64	4.10	5.61
	600	41.40	6.59	2.10	11.40
	800	31.40	5.17	0.81	17.43
	1000	7.70	3.90	0.40	12.71
Mixture C	20	49.83	1.15	6.33	0.31
	400	42.78	2.14	3.59	1.87
	600	29.06	6.98	1.82	3.75
	800	22.97	4.58	0.80	7.13
	1000	5.99	1.90	0.28	9.44

If we express the correlation of the employed non-destructive and destructive methods, we will be primarily interested in, mainly from the point of view of the testing practice, the correlation between the non-destructive parameters and flexural strength or compressive strength respectively.

Table 13.5 describes the correlation relationships between destructive and acoustic non-destructive methods. It can be stated that the measured resonance frequencies of the specimens tested by the MLS and the impact-echo methods are in very good correlation - their correlation coefficient reaches the value 0.998.

Both test methods work in lower frequency areas (1 - 20 kHz). At the same time, they are in very good correlation with the development of compressive strength and reach the values 0.960 for impact-echo and 0.948 for MLS.

In contrast, the pulse-echo method reaches lower correlation values with the MLS method, the impact-echo methods and compressive strength. However, it is in good correlation with flexural strength with the value of the correlation coefficient of 0.972. The excitation of the test specimens with higher frequencies (above 20 kHz) therefore correlates more with the flexural strength.

Table 13.5. Correlation coefficients of used testing methods

	f_L	f_0	f_{PE}	f_c	f_{ct}
f_L	1.000	0.998	0.852	0.960	0.946
f_0	**0.998**	1.000	0.834	0.948	0.932
f_{PE}	0.852	0.834	1.000	0.871	0.972
f_c	**0.960**	**0.948**	0.871	1.000	0.937
f_{ct}	0.946	0.932	**0.972**	0.937	1.000

13.5. Conclusions

The used non-destructive acoustic methods allowed the tested material to be examined in a wide frequency domain using different methods. The Impact-echo method uses a single mechanical impulse transmitted by the impact of a mechanical hammer to obtain the frequency spectrum of the tested material. The Pulse-echo method using a generated frequency impulse. The MLS method uses a maximum length sequence that creates a frequency spectrum by averaging several dozens of responses of the test specimen to the transmitted signal over a short time interval. Using FFT, the signals were converted from the time domain to the frequency domain.

Thermally degraded concrete specimens of both mixtures exhibited a shift of the resonance frequencies into the lower frequency domain which correlated with the change in the specimens' strength. The difference between the correlation of the pulse-echo method with compressive strength and flexural strength is significant and the method cannot be considered equally suitable to the IE and MLS methods for estimations of compressive strength and flexural strength. Of all the test methods, however, it has the highest correlation with flexural strength, which can be considered a weakness of conventional plain concrete. Flexural strength of concrete of common composition reaches at most 10% of the compressive strength.

From the point of view of quantitative and qualitative evaluation of the degree of damage to the tested material, the employed methods seem to be an appropriate and progressive instrument. Testing using the MLS method can be seen as the next evolutionary step from the Impact and Pulse-echo methods, although it suffers from prototype imperfections in the selected assembly. In case of testing test specimens, it offers a very wide range of test parameters but may only be used for testing of the passage of the transmitted signal in the longitudinal direction. The Impact and Pulse-echo methods have been tested for a long time, are quick and verified even for testing on massive elements with only one accessible side of the construction. The entire MLS method has so far been only tested in the traditional assembly with the transmitter on one side of the test specimen and the receiver on the reverse side. For a wider use of this method, it will be necessary to verify its capabilities in other transmitter – receiver assemblies as well as on more massive elements. However, the MLS method can provide higher resolution and sharpness of the response of the tested material than the Impact and Pulse-echo methods. It is therefore desirable to further develop this method and optimize it for diagnostic practice.

It should also be noted that the concrete used for construction purposes is mainly in the form of reinforced concrete. The interpretation of vibro-acoustic

measurements of temperature-degraded reinforced concrete is, however, a much more demanding discipline, which is not the subject of this chapter.

Acknowledgement

This work has been supported out under the project GAČR No. 16-02261S supported by Czech Science Foundation.

References

Bodnárová, L., Z, J., Hroudová, J. and Válek, J. (2013) Methods for Determination of the Quality of Concretes with Respect to their High Temperature Behaviour. doi: 10.1016/j.proeng.2013.09.040.

Carbol, L., Martinek, J. and Kusák, I. (2015) Influence of Water Content on Fundamental Frequency of Mortar Sample. doi: https://doi.org/10.4028/www.scientific.net/AMR.1124.273.

Carbol, L. (2016) 'Měření akustických vlastností stavebních materiálů pomocí pseudonáhodné sekvence', Czech Republic, PhD thesis. Brno University of Technology. [in czech]

Carino, N. (2001) 'The impact-echo method: an overview', in 2001 Structures Congress & Exposition. doi: 10.1061/40558(2001)15.

Domain, F. (2007) 'Engineering Analysis', Engineering Analysis. doi: 10.1201/9781420049619.

Lam, F. K. and Hui, M. S. (1982) 'An ultrasonic pulse compression system for non-destructive testing using maximal-length sequences', Ultrasonics, 20(3), pp. 107–112. doi: 10.1016/0041-624X(82)90070-1.

Lexcellent, C. (2017) Linear and non-linear mechanical behavior of solid materials, Linear and Non-linear Mechanical Behavior of Solid Materials. doi: 10.1007/978-3-319-55609-3.

Malhotra, V. M. and Carino, N. J. (2004) Handbook on Nondestructive Testing of Concrete, Handbook on Nondestructive Testing of Concrete.

Ongpeng, J. M. C., Oreta, A. W. C. and Hirose, S. (2015) 'Non-linear ultrasonic test for fiber-reinforced concrete using 3rd harmonic generation', in IABSE Conference, Nara 2015: Elegance in Structures - Report.

Potchinkov, A. (2005) 'Digital signal processing methods of global nonparametric frequency domain audio testing', Signal Processing, 85(6), pp. 1225–1254. doi: 10.1016/j.sigpro.2004.12.007.

Zhao, J. et al. (2014) 'A meso-level investigation into the explosive spalling mechanism of high-performance concrete under fire exposure', Cement and Concrete Research, 65, pp. 64–75. doi: 10.1016/j.cemconres.2014.07.010.